A Low-Cost Optical Sensor for Noncontact Vibration Measurements

Guido Perrone, *Member, IEEE*, and Alberto Vallan

***Abstract*—This paper presents a new noncontact method to measure vibrations by using a low-cost optical approach that is able to provide a submicrometer resolution. The transducer exploits a simple optical setup based on an intensity-detection scheme that is implemented with plastic optical fibers, whereas innovative nondemanding spectral data processing allows compensation of the vibrating surface reflectivity and the gains of the measurement chain. The performance of the proposed system has been assessed, through comparison with other techniques, by performing several measurement tests that use targets vibrating at frequencies from a few hertz up to several tens of kilohertz and with different values of reflectivity.**

***Index Terms*—Optical fibers, optical sensors, plastic optical fibers (POFs), vibration measurements, vibrometers.**

I. Introduction

THE PROBLEM of measuring vibrations is a very important topic that encompasses different areas of civil and industrial engineering. Some vibrations are intentional and necessary for the proper functioning of devices (e.g., shakers, ultrasonic cleaning baths, rock drills, etc.), whereas the others are just unwanted effects due to manufacturing tolerances or the response of the structure to external stresses. Therefore, a large number of methods to measure the frequency and/or the amplitude of the vibration using mechanical, electrical, or optical devices have been proposed in the literature [1], [2]. However, regardless of the working principle, these approaches can be subdivided into two broad categories, depending on the necessity of the physical contact with the vibrating object or not. Generally, contact sensors, such as strain gauges and piezoelectric accelerometers, are less expensive but can only be used for bulky vibrating objects to minimize their influence on the measurement, although the progress in micro/nanomachining is continuously reducing the size constraint that makes sensor perturbation negligible. For example, microelectromechanical systems (MEMS)-based accelerometers are emerging as very popular and cheap devices that are also suitable for consumer applications. However, despite their excellent characteristics, in many cases of practical interest, the contact sensors cannot be used either because of the difficulty of reaching the vibrating object or because of its extremely small size. Profiling the deformation of ultrasonic transducers or—more generally—measuring the vibration in a localized tiny spot, up to several tens of kilohertz, with micrometer displacements, are typical examples of where contact sensors are not effective. Optics provides excellent technologies to overcome these limitations, allowing the development of high-performance noncontact sensors, namely, the most interesting since they truly do not perturb vibrations. Many optical approaches have been proposed in the literature, the most popular being the interferometric method and the laser Doppler vibrometer (LDV). In interferometric methods, a laser signal beam is directed onto a moving target, and the back-reflected light is recombined with part of the incident light using different schemes (e.g., Michelson or Mach–Zendher schemes) [2]. The interferometers are characterized by very high performances in terms of resolution and bandwidth but are also very expensive and impose stringent mechanical requirements because alignment is critical. The laser vibrometers exploit the Doppler effect [3] to measure the frequency of a vibration; the amplitude is then recovered by the integration of the velocity, and thus, it may not be accurate enough for the precise measurement of very small displacements. Typically, a helium–neon or argon ion laser with a power of 10 mW to 20 W is used to obtain high signal-to-noise ratios, which may pose some limitations in the general usage, given the safety requirements. The LDVs can be used to measure both translational and torsional vibrations and are characterized by a very-high-frequency response, but the accuracy is highly dependent on the alignment between the emitted and reflected beams. However, the main limitation to their wide spreading comes from their cost: although some laser vibrometers are commercially available as a portable device, they are still quite expensive. Moreover, they are very sensitive to environmental conditions such as variations of temperature or fluctuations in the air flow between the instrument and the target, as can occur in industrial applications. Alternative, cheaper optical solutions using glass fiber bundles have been proposed [5]; in this case, some of the fibers in the bundle illuminate the target, some other fibers collect the back-reflected light, and the amplitude of vibration is recovered from the measurement of the intensity-modulated back-reflected light. This approach can give very good results, but being based on amplitude variations, it is also sensitive to the reflectivity of the vibrating surface and to the gains of the measurement chain. The compensation for the surface reflectivity has been addressed in [6] by using several receiving fibers, but it requires a proper calibration of the sensor.

An alternative method is proposed in this paper, where we present a high-resolution and cheap optical sensor to measure

Manuscript received June 30, 2008; revised September 10, 2008. First published December 16, 2008; current version published April 7, 2009. The Associate Editor coordinating the review process for this paper was Dr. Sergey Kharkovsky.

The authors are with the Dipartimento di Elettronica, Politecnico di Torino, 10129 Torino, Italy (e-mail: alberto.vallan@polito.it).

Color versions of one or more of the figures in this paper are available online at http://ieeexplore.ieee.org.

Digital Object Identifier 10.1109/TIM.2008.2009144

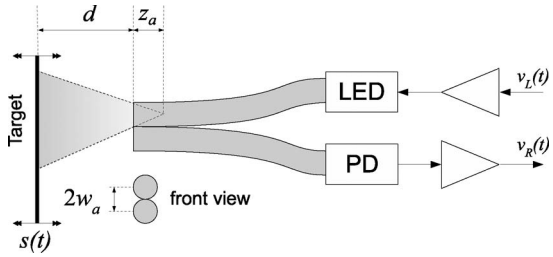

Fig. 1. Sketch of the sensor layout.

vibrations of up to several tens of kilohertz by using an intensity-detection scheme followed by innovative nondemanding data processing to compensate for the vibrating surface reflectivity and measurement chain gains. The setup is based on the detection of a modulated noncoherent beam of light generated by a light-emitting diode (LED) that is delivered to and from the analyzed surface by plastic optical fibers (POFs). The POFs permit the realization of a remote-sensing head without the complications and costs of glass fibers thanks to their superior light-collecting capability that translates into an overall ease of handling. The POFs typically have a 0.98-mm core (which is much larger than the 9-μm core of glass single-mode fibers used for high-performance optical communications and the 62.5-μm core of multimode glass fibers) that is made of Poly-Methyl-Methacrylate (PMMA) and surrounded by a thin (about 20 μm) fluorinated polymer cladding. The large core size, together with the high numerical aperture (about 0.5), accounts for a series of advantages of the POF over glass fibers and, most notably, easier connectivity, less attention to tolerances with a subsequent reduction in the connector requirements and costs, possibility to use low-cost transceivers based on LED instead of laser diodes, enhanced flexibility to shock and vibration thanks to a lower Young's modulus, etc. The POFs also exhibit some disadvantages, such as much larger attenuation and dispersion, but these drawbacks are of negligible impact for the sensing applications, specifically for those addressed in this paper.

The remainder of this paper is organized as follows. In Section II, we describe the working principle of the developed sensing system, and in Section III, we present the technique proposed to compensate for the variations in the surface reflectivity. Then, in Section IV, we analyze the sensitivity and uncertainty of the sensing system, and in Section V, we present the assessment of the performances through some experimental results achieved in different working conditions. Finally, in Section VI, we draw our conclusions.

II. Sensor Working Principle

The sensing head is made by two POFs with the radius w_a and the separation between the two axes $2w_a$, as shown in Fig. 1. One fiber is used to transmit the light from a noncoherent source (LED) driven by a transconductance amplifier, whereas the other fiber collects the light reflected by the target whose vibrations $s(t)$ have to be measured. The target distance from the fiber tips is d. An alternative and further miniaturized sensing head uses the same fiber both to deliver and collect the light beams, with the addition of a coupler to separate these

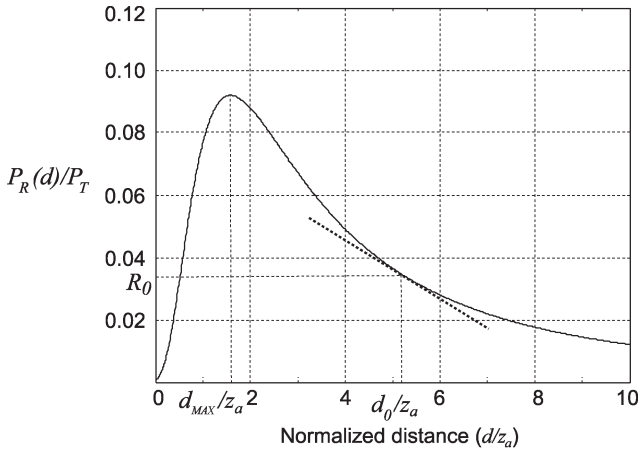

Fig. 2. Typical dependence of the power ratio with the normalized distance.

two signals. At the receiver side, a photodiode (PD) that is connected to a transimpedance amplifier is used to convert the light into an electric signal $v_R(t)$, which may be written as

$$v_R(t) = A \cdot v_L(t) \cdot \frac{P_r(d)}{P_t} \tag{1}$$

where $v_L(t)$ is the voltage applied to the LED driver, $P_r(d)/P_t$ is the ratio between the optical powers at the receiver and at the transmitting fiber surfaces, and the term A takes into account all the factors independent from d, such as the amplifier gains, the fiber and connector losses, the PD responsivity, and the target reflectivity.

The target vibrations modify the distance between the fiber tips and the target itself and, therefore, the received optical power $P_r(d)$. The exact relationship between the target position and the received power depends on the fiber characteristics, such as the numerical aperture, the core radius, the fiber surface polishing, and on the target surface. In the case of a reflective surface and a Gaussian beam, the received optical power can analytically be obtained as a function of the target distance d, of the fiber radius w_a, and of the position of the light asymptotic cone vertex z_a as [4]

$$\frac{P_r(d)}{P_t} = \frac{2}{\zeta^2} e^{-8/\zeta^2} \tag{2}$$

where $\zeta = 1 + 2d/z_a$. Fig. 2 shows an example of the typical measured behavior of the power ratio versus the distance; the maximum of the received optical power is for $\zeta = \sqrt{8}$, that is, for

$$d_{\mathrm{MAX}} = \frac{\sqrt{8} - 1}{2} z_a. \tag{3}$$

The power monotonically increases for a normalized distance that is lower than d_{MAX}, and then at larger distances, it reduces approximately like $1/d^2$, as expected from the theoretical considerations. Although the value of z_a could be computed from the *a priori* knowledge of all the parameters affecting the received power versus distance relationship, it is more practical to determine it from a measurement of this curve, given the difficulty to quantitatively evaluate some of these parameters,

such as the surface quality, the polishing angle of the fiber tip, etc. Considering a standard POF, the maximum received power is for a target distance that is close to about 1.6 mm so that $z_a \cong 1.75$ mm.

The target displacements $s(t)$ due to the vibrations behave like small changes of the target distance from the fiber tips $d(t) = d_0 + s(t)$, where d_0 is the mean value of the target distance. Therefore, the ratio P_r/P_t can locally be approximated at around d_0 as (straight dotted line in Fig. 2)

$$\frac{Pr(d)}{Pt} \simeq R_0 + R_1 \cdot (d - d_0) \tag{4}$$

which can be rewritten as

$$\frac{P_r(t)}{P_t} \simeq R_0 + R_1 \cdot s(t) \tag{5}$$

and therefore, the detected signal can be expressed as

$$v_R(t) = A \cdot v_L(t) \cdot (R_0 + R_1 \cdot s(t)). \tag{6}$$

The coefficients R_0 and R_1 that are involved in the linear approximation can analytically be evaluated from the optical power [see (2)] and its first derivative [see (10), shown below], which are both computed at the target mean distance d_0.

If the LED stimulus $v_L(t)$ is constant, then the received signal contains an ac component that represents the vibration $s(t)$ with a scale factor that depends on the first derivative R_1 of the curve in Fig. 2 and on the coefficient A. The former can analytically be evaluated provided that the working distance is either known or it can somehow be estimated, for example, by adding another receiving fiber to the sensing head. The term A depends on the chain gains and on the target reflectivity, which, in general, are both not known and, furthermore, may change with time.

III. Reflectivity Compensation Technique

The solution proposed in this paper is rather different from what has already been presented [5], and it is based on the spectral analysis of the received signal upon the sinusoidal modulation of the incident light $v_L(t) = A_0 + A_L \cdot \sin(\omega_L t)$. When the vibration $s(t) = A_V \cdot \sin(\omega_V t)$ is also sinusoidal, the received signal becomes

$$\begin{aligned} v_R(t) = {} & \underbrace{A \cdot A_0 \cdot R_0}_{\mathrm{V_0}} + \underbrace{A \cdot A_0 \cdot A_V \cdot R_1}_{\mathrm{V_1}} \cdot \sin(\omega_V t) \\ & + \underbrace{A \cdot R_0 \cdot A_L}_{\mathrm{V_2}} \cdot \sin(\omega_L t) \\ & + \underbrace{A/2 \cdot R_1 \cdot A_V \cdot A_L}_{\mathrm{V_3}} \cdot \cos[(\omega_L - \omega_V)t] \\ & + \underbrace{A/2 \cdot R_1 \cdot A_V \cdot A_L}_{\mathrm{V_4}} \cdot \cos[(\omega_L + \omega_V)t]. \end{aligned} \tag{7}$$

In this case, the target behaves like a mixer for the optical beams; therefore, the received signal has five spectral components, as shown in Fig. 3, each depending on the unknown term A. Thus, to determine the amplitude of the vibration A_v independently from A, in principle, it is sufficient to consider the ratio of any term containing A_V with a term not containing A_V; however, from a practical point of view and to also compensate the amplitude fluctuations of the LED emissions, there are only two possible solutions.

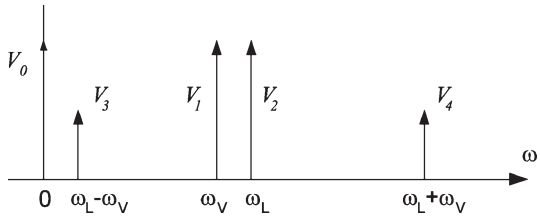

Fig. 3. Representation of the spectral components of the detected signal upon sinusoidal light modulation.

1) The vibration amplitude is obtained as the ratio of the component at the vibration frequency and the dc component. This solution is easier to implement when dealing with low-frequency vibrations, but it may introduce relevant disturbances since the dc component can be affected by the errors due to the ambient light and the offsets and drifts of the electronic circuitry.
2) The vibration amplitude is obtained as the ratio of the component V_2 and the component at the LED signal frequency V_3. This solution only involves ac components, which avoids the disturbances due to the dc term. Moreover, working with a high LED modulation frequency allows moving the beat signal V_3 (i.e., the component that is proportional to the vibration amplitude) farther away from the disturbances related to the mains signals, which thus improves the overall accuracy. In addition, choosing an LED modulation frequency that is close to that of the vibrating target, it is possible to take advantage of the mixing effect when measuring the high-frequency vibrations and shift down the beat signal at a frequency low enough to also be measured with low-performance devices. Moreover, with some limitations in the vibration bandwidth [7], this technique can also be employed to measure the nonsinusoidal vibrations converted to low frequencies.

Using the approach that only involves ac components, the amplitude of the vibration signal can be obtained by measuring the amplitude of the components V_3 and V_2 at the beat frequency $\omega_L - \omega_V$ and at the LED stimulus frequency ω_L, respectively. The vibration amplitude can thus be derived from (7) as

$$A_V = \frac{V_3}{V_2} \cdot \frac{2|R_0|}{R_1}. \tag{8}$$

The ratio between the spectral components compensates for the possible time variations of the target reflectivity or the amplifier gains, whereas the ratio $|R_0|/R_1$ acts as a scale factor that can analytically be computed from the fiber characteristics and the target distance using (2) and (10) obtained from the theoretical model

$$\frac{|R_0|}{R_1} = R_{01}(d_0) = \frac{\zeta(d_0)^3}{16 - 2\zeta(d_0))^2} \frac{z_a}{2}. \tag{9}$$

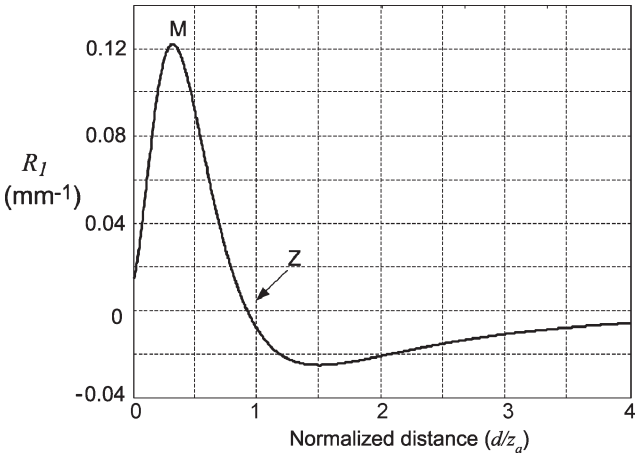

Fig. 4. Sensitivity as a function of the target normalized distance.

Relying on the theoretical model to compute the scale factor, it is possible to measure the vibration amplitude without the need for calibrations. However, in the presence of a diffusive target like in the test sets described in Section V, the optical behavior of the sensing systems can be significantly different from the model represented by (2). In these cases, a better performance can be achieved by only taking into account the real optical behavior of the sensing systems through the experimental determination of the $P_r(d)/P_t$ relation.

IV. Sensitivity and Uncertainty Analysis

The value of the fiber-to-target distance d_0 strongly affects the sensor behavior since it influences both the sensitivity and the metrological performance.

The sensitivity is directly proportional to the terms included in V_3, namely, A, R_1, and V_L. Therefore, the sensitivity can be improved by increasing the values of A and V_L when possible (i.e., using a high reflectivity target and a high LED driving current) and maximizing R_1, which is the first derivative of the optical power that is dependent on the distance d as

$$R_1(d) = \frac{\partial P_r/P_t}{\partial d} = R_0 \cdot \left(\frac{16}{\zeta^3} - \frac{2}{\zeta}\right) \cdot \frac{2}{z_a}. \qquad (10)$$

A typical behavior of R_1 with distance is shown in Fig. 4 considering the same POF used in Section II.

The sensitivity is highest for a normalized distance of about $d/z_a = 0.3165$ (point M) and is zero (point Z) when the optical power is at its maximum, that is, for $d = d_{\mathrm{MAX}}$.

However, in this application, where the target distance must be known to measure the vibration amplitude using (8), it is also important to minimize the uncertainty of the scale factor R_{01}. This uncertainty depends on the target distance d_0, on z_a, and on the model uncertainty that is due to the deviations of the physical behavior from the theoretical model described in (2). The latter accounts for several factors like the nonuniform reflectivity of the surface, the uncontrolled angle between the fiber tips and the target, the roughness of the fiber tips, etc. Since some of these terms depend on the specific sensor arrangement, a quantitative evaluation will empirically be provided in Section V-B.

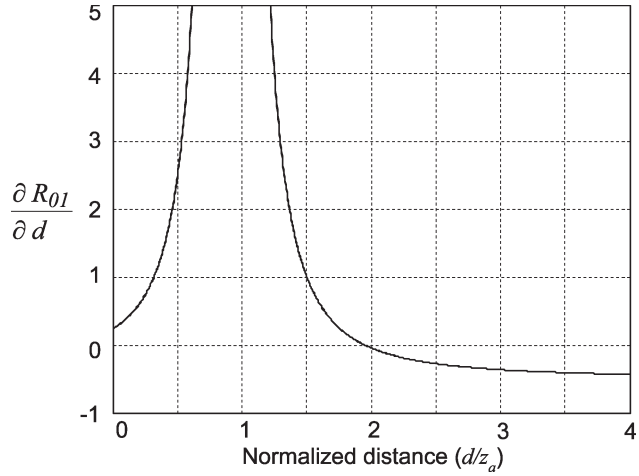

Fig. 5. Sensitivity of the scale factor with the target distance.

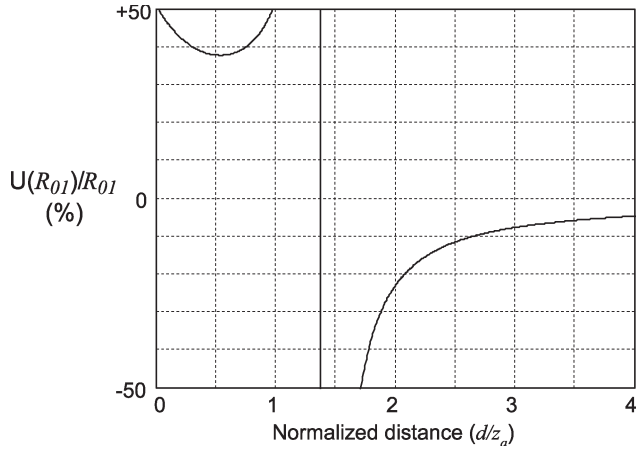

Fig. 6. Extended relative uncertainty of the scale factor R_{01}.

The effect of the distance d_0 on R_{01} can be obtained by using the common uncertainty propagation rules [8]. The sensitivity of R_{01} with the target distance d can, therefore, be analytically expressed as

$$\frac{\partial R_{01}}{\partial d} = \frac{48\zeta^2 - 2\zeta^4}{(16 - 2\zeta^2)^2}. \qquad (11)$$

The R_{01} sensitivity behavior is shown in Fig. 5, where it is possible to notice that the highest sensitivity is for small target distances, whereas for a normalized distance of about $d/z_a \cong 2$, the sensitivity is zero. This means that around this point, the scale factor uncertainty does not depend—at least to a first approximation—on the uncertainty of the distance d_0, which can, therefore, be known in an approximate way.

However, the scale factor R_{01} also depends on z_a, which is related to the fiber geometrical and optical characteristics, and that can be either computed or measured using (3). Fig. 6 shows the relative extended uncertainty $(k = 2)$ of the scale factor for $z_a = 1.75$ mm and when both of the standard uncertainties of d_0 and z_a are equal to 0.1 mm.

It is evident from Fig. 6 that, to reduce the uncertainty due to the scale factor, one should work at long distances, although in this range, the signals are small, thus increasing the uncertainty

due to the measurement of the spectral components in (8). In other words, the sensor working position has to be chosen as a compromise between the sensitivity and the uncertainty since they both increase for short distances.

V. Experimental Results

Different types of tests were carried out with a twofold objective: 1) Assess the performances of the proposed system by comparing the readings with those obtained from other devices or technologies; and 2) evaluate its applicability in conditions of practical relevance from the point of view of perspective applications. These tests include the following:

1) the verification of the reflectivity compensation technique by using a vibrating target having the surface of different colors and kept at a constant distance from the sensing head;
2) the comparison of the readings with those achievable from a commercial calibrated accelerometer under constant reflectivity but varying target distance conditions;
3) the determination of the resolution by using as a reference a precision computer-controlled micropositioning device;
4) the assessment of the high-frequency measurement capabilities by using a piezoelectric ultrasonic transducer driven at about 40 kHz.

The last two tests have already been described in [9], whereas the others have been extended or added in this paper and are, therefore, presented in detail in the following.

The sensing system arranged for the tests made use of a 670-nm LED and a PD, both having a bandwidth of 10 MHz and equipped with standard SMA connectors for POF. About 2 m of SI-PMMA POF with a core diameter of 0.98 mm was employed to fabricate the sensing head. The LED driver and the PD amplifier were custom-made circuits designed to have suitable gains and a bandwidth greater than 1 MHz. The commercial signal generators were employed to generate the drive signals for the LED and the vibration actuators used in the different experiments. The detected signal was acquired by using a digital acquisition board having a 16-bit resolution. The acquired signals were then processed by a PC using a fast Fourier transform (FFT) algorithm to extract the spectral component amplitudes.

A. Reflectivity Compensation

To verify the effectiveness of the proposed compensation technique, tests were carried out by employing a small loudspeaker as a vibrating target. A tiny piece of paper was glued in the middle of the moving coil and then painted with various colors so that the reflected optical power from the least reflecting paper was five times smaller than that measured in the case of the most reflecting one (white color).

The LED and the loudspeaker were driven with sinusoidal stimuli at 600 and 370 Hz, respectively. The received signal was amplified and then acquired by means of an acquisition board whose sampling rate was set to 10 kHz. The acquired signal was processed to measure the amplitudes of the components V_2 at 600 Hz and V_3 at 230 Hz. Fig. 7 shows a detail of the arranged

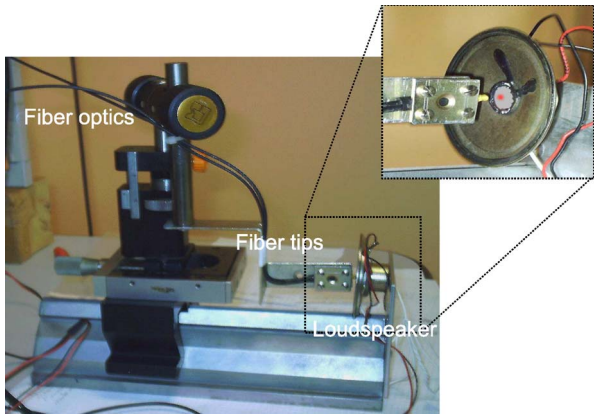

Fig. 7. Test set based on a loudspeaker used to assess the reflectivity compensation technique.

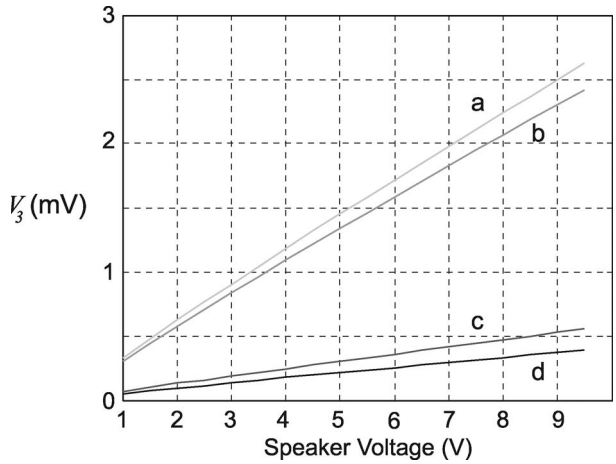

Fig. 8. Measured V_3 component amplitude for different values of reflectivity of the loudspeaker surface.

test set. The fiber tips were kept at a distance $d_0 = 5$ mm from the target, which is a value that represents a good compromise between sensitivity (which is high for small distances) and uncertainty (which reduces increasing the distance), according to the discussion in Section IV.

The speaker was driven at increasing current intensities to have different vibration amplitudes. Fig. 8 shows the measured amplitude of component V_3 for four different values of the surface reflectivity, which correspond to white, yellow, light blue, and dark gray, respectively. As is clearly evident, the amplitude of this spectral component is proportional to the vibration amplitude but is also strongly dependent on the surface reflectivity, as expected.

The vibration amplitude that was obtained by applying (8) to the components V_3 and V_2 is shown in Fig. 9, where it is possible to note that the curves show an excellent overlap that is only limited by factors such as the system reproducibility and the working distance uncertainty.

B. Comparison Tests With a Commercial Accelerometer

Comparative tests with a calibrated piezoelectric accelerometer were also performed to evaluate the response of the proposed sensor at a constant target reflectivity but at varying

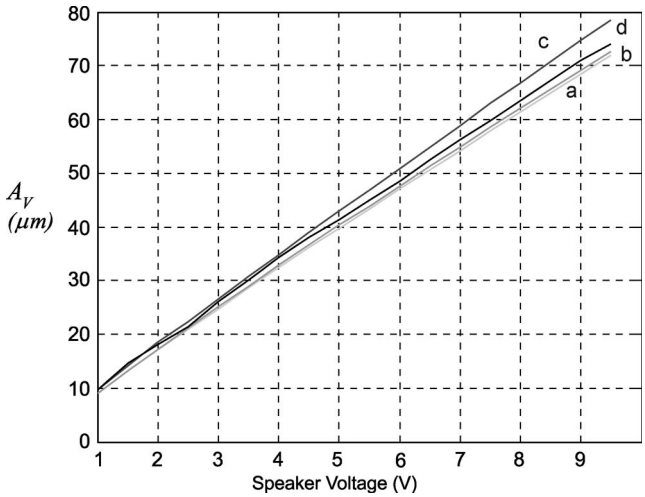

Fig. 9. Ratio amplitude between components V_3 and V_2 for a different value of reflectivity of the loudspeaker surface.

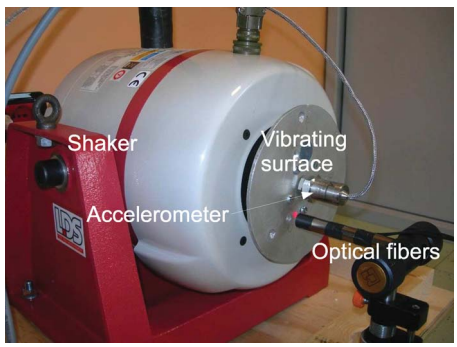

Fig. 10. Test set based on an electrodynamic shaker used in the comparisons with the calibrated accelerometer.

working distance conditions. An electrodynamic shaker was employed in this case to generate a steady sinusoidal vibration at $f_V = 1473$ Hz (Fig. 10). The fiber tips were placed in front of the shaker fixture as close as possible to the reference accelerometer. The LED modulation frequency was set to 10 kHz, and therefore, the beat component that is related to the vibration signal was at 8527 Hz. The choice of a high LED modulation frequency is useful to reduce the aliasing phenomena in the presence of distorted vibration signals, and it also avoids the interference of spurious optical signals due, for example, to fluorescent lights. The accelerometer output was acquired, and the spectral component at the vibration frequency was extracted; then, the vibration amplitude was obtained as $A_V^{\mathrm{acc}} = a/(2\pi f_V)^2$, where a is the peak value of the acceleration. The recovered peak of the vibration amplitude was $A_V^{\mathrm{acc}} = 3.2$ μm with a standard uncertainty of about 5% mainly due to the accelerometer frequency response.

The distance z_a was evaluated from the optical power curve, obtaining $z_a = 1.75$ mm with a standard uncertainty of about 0.1 mm. Then, this value was employed to derive the scale factor R_{01} from (9).

The results of the comparisons are reported in Fig. 11. The readings from the proposed sensor (curve a, together with its uncertainty band obtained with a coverage factor $k = 2$) show

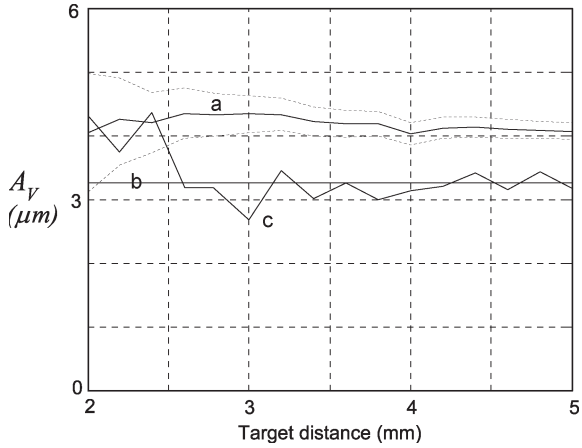

Fig. 11. Vibration amplitude measured at different target distances. (a) POF sensor with scale factor computed from the theoretical model of the optical link. (b) Amplitude obtained by processing the accelerometer output. (c) POF sensor with the scale factor empirically evaluated.

that the measured vibration amplitude is almost independent of the distance. However, it is possible to note a relevant difference between this curve and that obtained from the accelerometer (curve b, without the uncertainty band for clarity of the picture). This discrepancy can be ascribed to the use of the theoretical model to compute the scale factor R_{01}. This difference is reduced by using in (8) the empirical scale factor computed from the measured optical power R_0 and its first derivative R_1 (curve c). Therefore, in this application, the error due to the simplifications that are intrinsic in the theoretical model is not negligible with respect to the distance uncertainty. Anyway, it is important to highlight that curve a is compensated both for the reflectivity of the target surface and for the gains of the measurement chain, even if it has been obtained without any calibration of the sensor. On the other hand, curve c requires a calibration after the optical sensor fabrication.

VI. Conclusion

An innovative and low-cost system that measures vibrations using a noncontact approach, independent from the vibrating surface reflectivity, has been proposed and experimentally evaluated. The system uses POFs for the realization of the sensing head and a simple spectral analysis to evaluate the amplitude of the vibrations, compensating for the target reflectivity and offsets and gains in the measurement chain. A number of experiments to assess the performance of the developed system have been carried out by using vibrating surfaces with different values of reflectivity and frequency ranging from a few hertz to several tens of kilohertz. Comparisons with other techniques or reference systems have shown the capability of the system to measure the amplitude of vibrations up to about 40 kHz with a resolution of below 1 μm.

References

[1] P. M. B. S. Girao, O. A. Postolache, J. Faria, and J. M. C. D. Pereira, "An overview and a contribution to the optical measurement of linear displacement," *IEEE Sensors J.*, vol. 1, no. 4, pp. 322–331, Dec. 2001.

[2] S. Donati, *Electro-Optical Instrumentation: Sensing and Measuring With Lasers*. Upper Saddle River, NJ: Prentice–Hall, 2004.

[3] P. Castellini, M. Martarelli, and E. P. Tomasini, "Laser Doppler vibrometry: Development of advanced solutions answering to technology's needs," *Mech. Syst. Signal Process.*, vol. 20, no. 6, pp. 1265–1285, Aug. 2006.
[4] J. B. Faria, "A theoretical analysis of the bifurcated fiber bundle displacement sensor," *IEEE Trans. Instrum. Meas.*, vol. 47, no. 3, pp. 742–747, Jun. 1998.
[5] R. Dib, Y. Alayli, and P. Wagstaff, "A broadband amplitude-modulated fibre optic vibrometer with nanometric accuracy," *Meas.*, vol. 35, no. 2, pp. 211–219, Mar. 2004.
[6] X. Li, K. Nakamura, and S. Ueha, "Reflectivity and illuminating power compensation for optical fibre vibrometer," *Meas. Sci. Technol.*, vol. 15, no. 9, pp. 1773–1778, Sep. 2004.
[7] L. Schnell, Ed., *Technology of Electrical Measurements*. Chichester, U.K.: Wiley, 1993.
[8] *Guide to the Expression of Uncertainty in Measurement*, Int. Stand. Org., Geneva, Switzerland, Oct. 1993.
[9] A. Buffa, G. Perrone, and A. Vallan, "A plastic optical fiber sensor for vibration measurements," in *Proc. IEEE IMTC*, Vancouver, BC, Canada, May 12–15, 2008, pp. 1387–1391.

Guido Perrone (M'97) was born in Italy in 1965. He received the Ph.D. degree in electromagnetics from Politecnico di Torino, Torino, Italy.

He is currently with Politecnico di Torino, where he is lecturing on optical components and fibers and on microwave devices. His research activity is mainly in the fields of fiber optical sensors and high-power fiber lasers.

Dr. Perrone is member of the IEEE Microwave Theory and Techniques Society (MTTS), the IEEE Lasers and Electro-Optics Society (LEOS), and the Optical Society of America.

Alberto Vallan was born in Italy in 1967. He received the M.S. degree in electronic engineering from Politecnico di Torino, Torino, Italy, in 1996 and the Ph.D. degree in electronic instrumentation from the University of Brescia, Brescia, Italy, in 2000.

He is currently an Assistant Professor with the Dipartimento di Elettronica, Politecnico di Torino. His main research interests are digital signal processing and development and characterization of sensors and instruments for industrial applications.